Petroleum 8 (2022) 552–566

Contents lists available at ScienceDirect

Petroleum

journal homepage: www.keaipublishing.com/en/journals/petlm

Effect of ammonium based ionic liquids on the rheological behavior of the heavy crude oil for high pressure and high temperature conditions

Sivabalan Sakthivel [a, *], Sugirtha Velusamy [b]

[a] Center for Integrative Petroleum Research (CIPR), College of Petroleum Engineering & Geosciences, King Fahd University of Petroleum & Minerals, Dhahran, 31261, Saudi Arabia
[b] Petroleum Engineering Program, Department of Ocean Engineering, Indian Institute of Technology Madras, Chennai, 600 036, India

ARTICLE INFO

Article history:
Received 21 May 2020
Received in revised form
20 September 2020
Accepted 22 June 2021

Keywords:
Crude oil
Ionic liquids
Loss modulus
Microscopy
Storage modulus
Viscosity reduction

ABSTRACT

Heavy crude oil (HCO) production, processing, and transportation forms several practical challenges to the oil and gas industry, due to its higher viscosity. Understanding the shear rheology of this HCO is highly important to tackle production and flow assurance. The environmental and economic viability of the conventional methods (thermal or dilution with organic solvents), force the industry to find an alternative. The present study was constructed to investigate the effect of eco-friendly ionic liquids (ILs) on the HCO's rheology, at high temperature and high pressure. Eight different alkyl ammonium ILs were screened for HCO's shear rheology at the temperatures of 25–100 °C and for pressures 0.1–10 MPa. The addition of ILs reduced the HCO's viscosity substantially from 25 to 33% from their original HCO viscosity. Also, it aids to reduce the yield stress to about 15–20% at all the studied experimental conditions. Furthermore, the viscoelastic property of the HCO was studied for both strain-sweep and frequency-sweep and noticed the ILs helps to increase HCO's loss modulus (G″) by reducing storage modulus (G′), it leads to the reduction of the crossover point around 25–32% than the standard HCO. Mean the ILs addition with HCO converts its solid-like nature into liquid-like material. Besides, the effect ILs chain length was also studied and found the ILs which has lengthier chain length shows better efficiency on the flow-ability. Finally, the microscopic investigation of the HCO sample was analyzed with and without ILs and witnessed that these ILs help to fragment the flocculated HCO into smaller fractions. These findings indicate that the ILs could be considered as the better alternative for efficient oil production, processing, and transportation.

1. Introduction

Two third of the depleted reservoir's trapped oil remains unrecovered even after primary and secondary recovery processes [1,2]. The complex nature of the heavy crude oil (HCO) burdens its production, processing, and transportation facilities by reducing its flow-ability [3]. Typically, the higher extent of resins and asphaltenes in the HCO, flocculation/aggregation occurs with the polar fraction of the remaining HCO and makes it further heavier. It affects their flowing capacity in different regimes of the oilfield industry, such as impeding the HCO mobility from reservoir to wellbore, deposition at near-wellbore (skin formation) during production, and pipeline deposition in the course of oil transportation [4–9]. According to the American Petroleum Institute (API), the oil which has the API gravity ≤ 10 is considered as non-mobilizable oil due to its heavily viscous nature. Hence, the upstream oil and gas industry are hassled to overcome multifaceted operational challenges due to the complex nature of the substituents present in HCO [10]. It is, therefore, essential to increase the flow capacity to a certain extent to enable flow assurance.

Rheology is the basic tool, which is being commonly used to understand fluid flow resistance and deformation of the matter. It is also used to measure the viscoelastic behavior of the fluid

* Corresponding author.
E-mail address: sivabalan.sakthivel@kfupm.edu.sa (S. Sakthivel).
Peer review under responsibility of Southwest Petroleum University.

Production and Hosting by Elsevier on behalf of KeAi

https://doi.org/10.1016/j.petlm.2021.06.002

properties, particularly during the amplitude sweep and frequency sweep. Measuring both the viscous, (storage modulus (G′)) and elastic (loss modulus (G″)) nature of the substance, is more important in the oilfield applications, which will be studied under extended temperature, pressure and salinity conditions, to mimic the realistic reservoir condition property. Based on these useful data, the hardcore fluid transportation, such as pipeline transportation through the sea, desert, etc., can be performed to ensure the regular flow when varying temperature and pressure between region to region as well as from surface to pipeline conditions.

Heat treatment, chemical methods such as dilution with light oil or solvents (toluene), emulsification with the assistance of the surfactants or polymers are the typical flow improving methods used by the upstream and downstream industry. The upstream production sector achieves good mobility of heavy and extra heavy crude oil by using steam injection and microbial flooding methods to reduce the oil viscosity [4,11–13]. Asphaltenes and resins in the HCO tend to lose their intramolecular interactions on increasing the system temperature and enabling better oil mobility towards the production well. The same phenomenon can assist the oil transportation facilities to reduce the oil viscosity and for ease of pumping. However, the main drawback of this method is the requirement of more heat energy generation and, consequently, tackling heat loss will be another tedious task due to non-uniform heat transportation within the reservoir, especially at long distance porous media/wellbore/pipelines [4,11]. In the case of the microbial enhanced oil recovery method, the long-chain hydrocarbon in the reservoirs tends to undergo degradation over time, when injecting the microorganism into the oil reservoir. After the saturation point, most of the lengthier chain hydrocarbons would be converted into short-chain hydrocarbon with lesser viscosity, which will be easier to flow through the porous media towards the production well. However, the stability of the microorganism is not that great at reservoir conditions, particularly at high temperature and high pressure [14]. Yet another alternative for these thermal/microorganism methods is emulsification, wherein the oil is dispersed in the continuous water phase, causing a reduction in the ratio of shear stress to a shear rate of non-Newtonian fluid (apparent viscosity). Typically, conventional surfactants are being used for these emulsification processes and, conversely, their stability is yet to be studied well, since most of the surfactants fail at reservoir conditions of high temperature, pressure, and salinity [9,11]. Though many researchers are still working on the development of novel surfactants that are stable at high-temperature high-pressure conditions, their scalability, retention, and cost of the surfactants remain unaddressed to date.

Ionic liquids (ILs) are organic molten salts with an organic cation and anion with poor coordination and they are found to be in a liquid state at/below 100°C [15,16]. They possess strong physicochemical properties such as, low melting point, non-flammability, negligible vapor pressure, etc., due to which they are studied in various sector of oil and gas industry, such as biomass conversion, bitumen recovery, asphaltenes degradation, pipeline deposition, bitumen recovery, desulphurization, etc [17–33]. Also, the ILs could be structure tuned based on the required physicochemical properties, by altering the chemical structure of cation and anion. Moreover, these ILs could be recycled using a minimum quantity of water and can be reused innumerable times. In our prior studies, we attempted to use different types of ILs for tank bottom sludge dissolution and oil/water interfacial alteration studies, in which we executed the recovery and re-usage of ILs number of possible times [20].

Recently, several researchers studied the possible applications of ILs in various areas of the oil and gas industry [6,17–20,22–33]. Asphaltenes dissolution using two imidazolium-based ILs, 1-butyl-3-methylimidazolium chloride ($[BMIM]^+[Cl]^-$) and 1-butyl-3-methylimidazolium aluminum tetrachloride ($[BMIM]^+[AlCl_4]^-$) have been studied and found that ILs aid to enhance the asphaltenes dissolutions more significantly with the minimal quantity of ILs [25]. Shaban et al. (2014) studied the heavy oil upgradation at high temperature (70–90°C) using ILs, $[BMIM]^+[Cl]^-$ and $[BMIM]^+[FeCl_4]^-$ and noticed a significant reduction of oil viscosity with the addition of IL, particularly the IL, $[BMIM]^+[FeCl_4]^-$ enhanced oil flow property more substantially than the other IL. Also, it was witnessed that ILs help to reduce the sulfur content (desulphurization) of the heavy oil, making possible interaction with the sulfur present in the heavy oil fraction and later weakening of the C–S bond and stronger interaction of the IL-S bond of the heavy oil fraction occurred [6].

In the same way, Painter et al. (2010) studied the use of some of the imidazolium-based ILs on the bitumen recovery process, in which the researcher studied the dissolution of bitumen with the addition of organic solvents with and without ILs and found the IL added system enhanced the bitumen solubility to a greater extent than the organic solvent alone system [22]. Similarly, the reduction of the oil viscosity was also studied few researchers, particularly the author Fan et al. (2007) studied the efficacy of the ILs, $[Et_3NH]^+[AlCl_4]^-$, $[Et_3NH]^+[AlCl_4]^-Ni^{2+}$, $[Et_3NH]^+[AlCl_4]^-Fe^{2+}$ and $[Et_3NH]^+[AlCl_4]^-Cu^+$ on the heavy oil viscosity at the room temperature condition and found significant improvement of the heavy oil flowability with the addition of ILs. Noticeably the IL, $[Et_3NH]^+[AlCl_4]^-Ni^{2+}$ found to be more prominent among the studied ILs. Additionally, these ILs also reduced the asphaltenes content substantially [25]. It would have been more useful if the author could have conducted these experiments at high pressure and high temperature to understand their efficiency at the reservoir condition. Hu and Guo (2005) studied for the first time, the effect of some pyridinium ILs for asphaltenes dissolution, wherein the author studied the effect of alkyl chain length as well as the effect of various anionic species and their charge densities. It has been experimentally witnessed that the ILs with a higher charge density of anion with a lower charge density of the cation was found to be more efficient to reduce the asphaltenes precipitation (asphaltenes dissolution) [34]. Also, it is being observed better efficiency with a higher concentration of the ILs (0.5–5 wt%) on the reduction in asphaltenes precipitation, however, a high concentration of the ILs usage is not found to be economically viable. This may be attributed due to the more/sufficient number of ILs availability for the possible electrostatic interactions with asphaltenes moiety, which will reduce the asphaltenes aggregation structure more substantially.

In our recent past, we have studied a variety of ionic liquids from different groups, such as imidazolium, alkylammonium, hydroxyalkyl ammonium butyro lactam, and caprolactam for various applications like sludge/pipeline removal, oil/water interfacial reduction, corrosion inhibition, and wettability alterations, etc. It was noticed the lengthier alkyl chain and/or bulkier ring containing ILs works more efficiently in our studies [17–20,26–33]. Obviously, it was noticed very limited studies on the evaluation of ILs on the heavy oil's rheology characteristics. It is being witnessed from the literature review, that ILs have the capability to improve the flowability of the heavy crude oil. However, most of these studies were carried out under low temperature and pressure and failed to address the viscoelastic behavior of the heavy oil. To mimic the realistic reservoir condition, it is necessary to perform the experimental tests at high pressure and high temperature. In this regard, in the present study, we have attempted to study the effect of eight different alkyl ammonium-based ionic liquids on the viscoelastic (rheological) behavior of the heavy crude oil at high pressure and high temperature (HPHT). Particularly, this study aims to

understand the viscoelastic behavior of heavy crude oil using amplitude sweep and frequency sweeps, such as storage modulus (G′) and loss modulus (G″) with and without the addition of ILs at various temperatures (25, 50, 343.15 and 100 °C) and pressures (0.1, 0.25, 0.5, 7.5 and 10 MPa). This study also investigates the effect of alkyl chain length and different anionic moieties of the ILs on the HCO rheological behavior. The concentration of the IL is set to be 5000 ppm based on the previous determination of critical micellar concentration [30]. In addition to this, the present study is also exploring the microscopic characterization of different ILs on the heavy crude emulsion. Understanding the rheology of this HCO with the addition of ILs would help to increase oil production as well as to improve the flow properties of the fluid.

2. Experimental section

2.1. Materials: heavy crude oil and ionic liquids

The present study uses heavy crude oil with the SARA composition of Saturates = 36.2%, Aromatics = 50.0%, Resins = 11.0%, Asphaltenes = 2.8%. The physicochemical properties of this heavy crude oil sample, such as API gravity, density, surface tension, and interfacial tension are summarized in Table 1.

The standard uncertainties are u(density) = 0.001 kg/m^3, u(surface/interfacial tension) = 0.03 mN/m.

In this study, there are *eight* different ammonium-based alkyl ammonium ionic liquids synthesized based on the existing literature [35], with the simple acid-base neutralization approach and studied their effect on the heavy crude oil rheology. They are listed in Table 2 as, namely, Diethylammonium phosphate $[Et_2NH_2]^+[H_2PO_4]^-$, Diethylammonium sulfate $[Et_2NH_2]^+[HSO_4]^-$, Triethylammonium acetate $[Et_3NH]^+[CH_3COO]^-$, Triethylammonium tetrafluoroborate $[Et_3NH]^+[BF_4]^-$, Triethylammonium phosphate $[Et_3NH]^+[H_2PO_4]^-$, Triethylammonium sulfate $[Et_3NH]^+[HSO_4]^-$, Tripropylammonium sulfate $[Pr_3NH]^+[HSO_4]^-$ and Tributylammonium sulfate $[Bu_3NH]^+[HSO_4]^-$. Prior to use, the synthesized ILs were purified/dried enough (up to 72 h) using the vacuum setup at the temperature of 353 K to ensure the ILs are free of impurities/moisture and were screened through ^{1}H nuclear magnetic resonance (^{1}H NMR: Bruker Avance 500 MHz spectrometers) spectroscopy using DMSO/$CDCl_3$ solvents to identify their chemical structures. Thereafter, Analab Karl Fischer Titrator was employed to quantify the water content of the synthesized ILs and found that it was below 1000 ppm for all the dried ILs. Subsequently, the surface and the interfacial phenomenon of the crude oil, IL solutions and oil/water systems were studied with the use of Dynamic Contact Angle Tensiometer (Dataphysics DCAT 11 EC, Germany), wherein the Wilhelmy platinum-iridium plate was used as the probe/sensor to measure the surface/interfacial tensions.

2.2. Rheological studies

2.2.1. Viscosity measurements

Anton Paar Modular Compact Rheometer (MCR 52, Physica, Austria) was employed to study the viscosity/rheological behavior of the heavy crude oil with and without ILs at various temperatures and pressures. A double gap geometric concentric cylinder measuring system (model no. DG35/26,483) was used as the sample holder to establish greater availability of contact area between the sample and the surface of the geometry, thereby, providing high torque resolution for the test. A hollow gap of the bigger cylinder accommodates the small hollow cylinder and the intermediate gap holds the sample. This system withstands a high temperature (>423 K) and high pressure (up to 40 MPa). The rheometer was fitted with an external water bath to circulate the fluid at the desired temperature condition. Prior to beginning the experiments, the geometry system was cleaned thoroughly using different solvents (water/toluene/acetone) to ensure no contamination. Meanwhile, the HCO or HCO + IL samples were homogenized (agitated with stirring as shown in Figure S1 for 2–3 h with a constant speed, 240–250 rpm at the atmospheric condition) before loading into the measuring system. Then, the desired experimental conditions of temperature and pressure were set and allowed to stabilize for 1 h.

Initially, the viscosity behavior of HCO samples at a varying shear rate (0.1–1000 s^{-1}) was screened with no ILs. For, this the known quantity (2.35 g) of standard heavy crude oil sample was placed into the double gap measuring geometry and sealed properly. The measuring system was then fit appropriately into the rheometer and the desired experimental condition of temperature and pressure was set for the system. Subsequently, this was performed at different temperatures (25–100°C) and pressures (0.1–10 MPa). Then, the different concentrations of ILs, such as, 0, 100, 250, 500, 5000, 10,000, 25,000 ppm with HCO was screened at various temperatures (25, 50, 75 and 100°C) and pressures (0.1, 2.5, 5, 7.5, 10 MPa). Based on this, the optimal IL concentration for the present study is set to be 5000 ppm., ie., 2.35 g of the HCO +11.75 mg of IL (0.5 wt% or 5000 ppm). Moreover, the used ILs were recycled as we discussed in our previous study and reused as well.

2.2.2. Viscoelastic measurements

Linear viscoelastic region (LVR) of the different fluid systems, such as HCO and HCO + ILs were obtained by performing the strain sweep measurements, by varying the strain amplitude from 0.1 to 100% with a fixed frequency of 10 rad s^{-1} [36]. Based on this, the critical strain can be identified, by observing the change of the storage modulus (G′) to non-linearity from linearity. Typically, the constant behavior of the G′ at varying strain amplitude can be considered as the linear viscoelastic region, and, in the region above, the G′ curve tends to decrease nonlinearly when increasing the strain amplitude [36]. Further, this linear viscoelastic region can be used as the input for the measurement of the storage and loss modulus of corresponding fluid systems in the frequency sweep test. In the frequency measurements, their strain amplitude was set to be constant (viscoelastic region) with the changes in the frequency from 0.1% to 100%. Due to the rheometer insensitivity below 1% of the strain/frequency sweep, all the results shown here start from 1% of strain/frequency sweep. Moreover, all the experiments shown here are repeated thrice to ensure reproducibility.

Table 1
Physicochemical properties of the heavy crude oil (HCO)$^+$.

No. of trials	Composition				Wax content (%)	Density at 25°C (kg/m^3)	API gravity	Water content (%)	Surface tension at 80°C (mN/m)	Interfacial tension with pure water at 80°C (mN/m)
	S (%)	Ar (%)	R (%)	As (%)						
1	36.2	50.0	11.0	2.8	11.86	0.9979	11.55	2.354	54.58	23.52

$^+$S: Saturates; Ar: Aromatics; R: Resins; A: Asphaltenes.

Table 2
List of studied ionic liquids for this investigation.

Cation	Anion	Name	Abbreviation
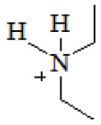	$[H_2PO_4]^-$	Diethylammonium phosphate	$[Et_2NH_2]^+[H_2PO_4]^-$
	$[HSO_4]^-$	Diethylammoniumsulfate	$[Et_2NH_2]^+[HSO_4]^-$
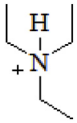	$[CH_3COO]^-$	Triethylammonium acetate	$[Et_3NH]^+[CH_3COO]^-$
	$[BF_4]^-$	Triethylammoniumtetrafluoroborate	$[Et_3NH]^+[BF_4]^-$
	$[H_2PO_4]^-$	Triethylammonium phosphate	$[Et_3NH]^+[H_2PO_4]^-$
	$[HSO_4]^-$	Triethyl ammonium sulfate	$[Et_3NH]^+[HSO_4]^-$
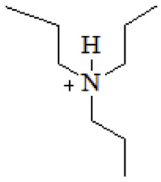	$[HSO_4]^-$	Tripropylammoniumsulfate	$[Pr_3NH]^+[HSO_4]^-$
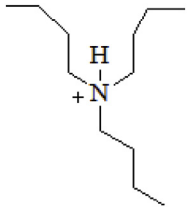	$[HSO_4]^-$	Tributylammoniumsulfate	$[Bu_3NH]^+[HSO_4]^-$

2.3. Morphological investigations

In addition to the rheological study, the simple microscopic investigation of the ionic liquids added oil emulsions (HCO + ILs) was analyzed using a high-resolution inverted microscope (Leica DMI3000B Inverted Microscope, Germany) to understand the morphological behavior of the HCO + IL systems. The complete set of this study was performed with a constant ratio of 1:0.1 of HCO:ILs (wt/wt %). This HCO + ILs mixture was homogenized thoroughly for 24 h using a magnetic stirrer agitator before they were subjected to optical microscopic analysis.

3. Results and discussion

This study aims to investigate the effect of ionic liquids on the shear rheological behavior of the HCO sample as a function of ILs concentration, temperature, and pressure. Initially, this section presents the discussion of shear rheological characterization of the HCO with and without ILs. Secondly, it deals with the viscoelastic properties of the HCO sample with and without ILs, such as yield stress, storage modulus (G′), and loss modulus (G″). Lastly, the microscopic investigation of HCO and HCO + IL systems were studied to support the effect of ILs on the HCO's rheological characteristics.

3.1. Shear rheological characterization

3.1.1. Standard heavy crude oil

Figure S2 shows the shear rheological behavior of the standard heavy oil sample at varying shear rate from 0.1 to 1000 s^{-1}, as a function of temperature (25–100°C) and pressure (0.1–10 MPa). Obviously, it is to be witnessed from Fig. S2, that this HCO behaves as a non-Newtonian shear-thinning fluid with a considerable reduction of the viscosity when increasing the shear rate irrespective of the temperature and pressure. However, an increase in the system pressure from 0.1 to 5 and 10 MPa causes a significant increment in the viscosity of the HCO system by reducing the fluid mobility. The viscosity of the neat HCO sample was found to be 17,203 cP at the temperature of 25°C, in 0.1 MPa (as shown in Table 3) and when increasing the system pressure to 10 MPa from 0.1 MPa, their viscosity has also been increased to 27,751 cP (61% increase). This increase in fluid viscosity on increasing system pressure is mainly attributed due to the reduction of the Brownian motion of the fluid's molecules at high pressure (N_2 gases would tend to occupy the empty spaces which were availed before, and now the system would behave to be tighter). Similar observations

Table 3
Viscosity data for HCO and HCO + ILs at the shear rate of 1 s^{-1}, as a function of pressure and temperature.

System	Pressure (MPa)	Temperature (°C)/Viscosity[a] (cP)			
		25	50	75	100
Heavy Crude oil (HCO)	0.1	17,203	1589	253	63
	5	22,555	2055	329	79
	10	27,751	2459	345	89
HCO+$[Et_3NH]^+[HSO_4]^-$	0.1	13,254	1289	210	53
	5	19,854	1604	278	58
	10	24,587	2015	295	61
HCO+$[Pr_3NH]^+[HSO_4]^-$	0.1	12,500	1265	204	52
	5	17,859	1548	261	56
	10	23,598	1985	288	60
HCO+$[Bu_3NH]^+[HSO_4]^-$	0.1	12,001	1165	198	50
	5	16,958	1458	245	52
	10	22,458	1895	265	55
HCO+$[Et_2NH_2]^+[H_2PO_4]^-$	0.1	14,754	1411	266	61
HCO+$[Et_2NH_2]^+[HSO_4]^-$	0.1	13,711	1355	245	58
HCO+$[Et_3NH]^+[CH_3COO]^-$	0.1	13,596	1328	234	58
HCO+$[Et_3NH]^+[BF_4]^-$	0.1	13,685	1345	236	56
HCO+$[Et_3NH]^+[H_2PO_4]^-$	0.1	13,459	1304	229	59

[a] = viscosity (at shear rate of 1.0 s^{-1}).

were found in other cases as well with an increase in system pressure. Similarly, the effect of temperatures was also screened from 25 to 100°C with a 25°C interval. It is to be noticed that neat HCO's viscosity has been declined more enormously when increasing system temperature from 25 to 100°C at a constant pressure of 0.1 MPa. For example, the standard HCO has been found to have the viscosity 17,214 cP at 25°C, when increasing the temperature to 50, 75 and 100°C, their viscosity has been reduced as 1589, 253 and 63 cP respectively (see Table 3). Typically, when increasing system temperature, their chemical bond length gets increased with increased vibrations, followed by which the physicochemical interactions between the oil molecules get suppressed, which means that the molecules get increased thermal energy and, thus, they are free to move faster than before. Also, the heavier fraction (high molecular weight compounds), such as asphaltene, resin, and bulkier aromatics will tend to lose their aggregation and this helps in the reduction of the viscosity and easy flow of the fluids [37]. Overall, the temperature and pressure dependency of the standard HCO is depicted in Fig. 1, for the constant shear rate of 1000 s^{-1}. Irrespective of the system temperature there is always a minor enhancement in the viscosity observed when increasing the system pressure as depicted in Fig. 1.

The standard uncertainties are $u(T) = 0.1$ K, $u(P) = 0.01$ MPa, $u(viscosity) = 2$ cP.

3.1.2. Effect of ILs on the viscosity of heavy crude oil

This study deals with the effect of eight different alkyl ammonium-based ionic liquids screened for the shear rheological property of HCO and validated their efficiency towards enhancing the flow property. In the beginning, one particular IL, $[Bu_3NH]^+[HSO_4]^-$ with HCO was studied with different concentration of IL, such as 0, 100, 250, 500, 5000, 10,000, and 25,000 ppm as shown in Figure S3, and from this, the optimum concentration of the IL has been set as 5000 ppm for the subsequent studies. Fig. 2 shows the effect of different cationic moieties of the ILs with the same anion, such as $[Et_3NH]^+[HSO_4]^-$, $[Pr_3NH]^+[HSO_4]^-$ and $[Bu_3NH]^+[HSO_4]^-$ on the shear rheological behavior of standard HCO. Wherein 5000 ppm of ILs was screened with standard HCO as a function of temperature (25, 50, 75 and 100°C) and pressure (0.1, 2.5, 5 and 10 MPa). It is noticed from Fig. 2, the addition of ILs reduces the HCO viscosity more significantly irrespective of the type of ILs, however, the lengthier alkyl chain containing ILs reduces the system viscosity to a greater extent than the other ILs. The addition

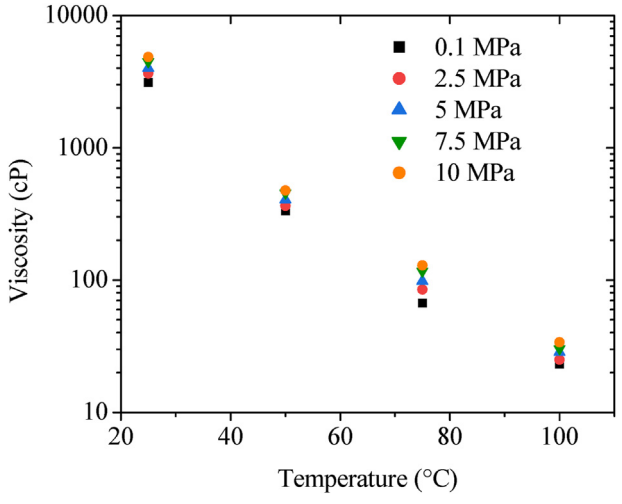

Fig. 1. Effect of temperature and pressure on the viscosity (at a shear rate of 1000 s^{-1}) of the standard HCO.

of ILs, $[Et_3NH]^+[HSO_4]^-$, $[Pr_3NH]^+[HSO_4]^-$and $[Bu_3NH]^+[HSO_4]^-$ with HCO reduced the oil's viscosities as 13,254, 12,500, 12,001 cP from the standard value of 17,203 cP at 25°C and 0.1 MPa (see Table 3). It can be noticed that the addition of ILs reduces the viscosity to around 23–30% from their original value. Besides, as expected the increase in system pressure increases the fluid viscosity and the increase of the system temperature decreases the fluid viscosity as discussed in the previous section. However, the reduction of viscosity is found to be more in lower pressure (0.1 MPa) and in higher temperatures (35,315-100°C) (see Table 3). Analogously, the effect of various anionic moieties of the ILs such as $[HSO_4]^-$, $[H_2PO_4]^-$, $[CH_3COO]^-$, $[BF_4]^-$ with the same cationic moiety $[Et_3NH]^+$, was also screened with standard HCO at 0.1 MPa in 25°C (see Table 3). It is to be noticed that the anionic species, $[HSO_4]^-$ works better than the other studied anions. The anions $[CH_3COO]^-$ and $[BF_4]^-$ show the least performance on the HCO viscosity reduction than the other two studied anions. Overall, it provides the trend as: $[HSO_4]^- > [H_2PO_4]^- > [CH_3COO]^- > [BF_4]^-$ for the measure of efficiency towards oil viscosity reduction. Moreover, Fig. 3, shows the overall comparison of all the eight various ILs on the reduction of HCO viscosity and their viscosity reduction percentage at the shear rate of 1000 s^{-1}, for different temperatures and pressures.

However, experimentally two major indications are being witnessed. Firstly, the longer chain containing ILs reduces the HCO viscosity more efficiently than the shorter chain containing ILs. This could be attributed due to the higher hydrophobic nature of the lengthier alkyl chain containing ILs ($[Bu_3NH]^+[HSO_4]^-$) than the shorter alkyl chain containing ILs ($[Et_3NH]^+[HSO_4]^-$). When increasing the hydrophobicity of the ILs, it would enhance the possible van der Waals force of interactions (London dispersion force) between alkyl chain of ILs with the alkyl chains of the crude oil moieties, which leads to the possible reduction of HCO aggregation of a heavier fraction of hydrocarbons, it is nonpolar-nonpolar interaction or miscibility [30]. Identically, there could also be a certain amount of polar-polar interaction possible between the polar part of ILs ($R_3NH]^+$) with the polar fraction of crude oils, such as asphaltene and resins (Heteroatoms such as N, S, O). This could inhibit the self-aggregation of the crude oils, such as asphaltene precipitation. Moreover, in general, longer chain containing polar ILs are found to be more suitable candidates to balance both the hydrophobic-hydrophobic interaction of HCO-IL system (alkylic hydrocarbon of HCO interaction with the alkyl moiety of ILs) and polar-polar interaction of HCO-IL system (HCO's asphaltene/resin interaction with charged species of IL). Secondly, it also depends on the anionic moiety of the ILs, wherein the ILs containing more charge density anions such as, $[HSO_4]^-$ are more prominent than the other anionic moieties. However, it is to be understood that the IL containing longer chain containing (hydrophobic) cation with the combination of higher charge density containing anions is the perfect choice for enhancing the flow property of HCO systems.

Basically, once the cation of the ILs gets developed interaction with the heteroatoms of the HCO (asphaltene/resin), ILs tend to retard the asphaltene aggregation (asphaltene precipitation) with another asphaltene/resin/heavier fraction of HCO, which means the other fractions of HCO such as saturates/aromatics are free for ease of flow. Mechanistically, the asphaltenes precipitation occurs mostly by the π-π stacking, electrostatic acid-base interaction and hydrogen bonding interaction between the crude oil systems, such as heteroatoms (-S and/or −N) of asphaltene/resin units trying to undergo the hydrogen bonding interaction with the other heavier fraction of HCO's (asphaltene/resin) alcoholic moieties, such as (-S—H—N-). With the addition of ILs, the anionic species of the ILs such as, $[HSO_4]^-$ tend to drawdown the hydrogen towards the anionic

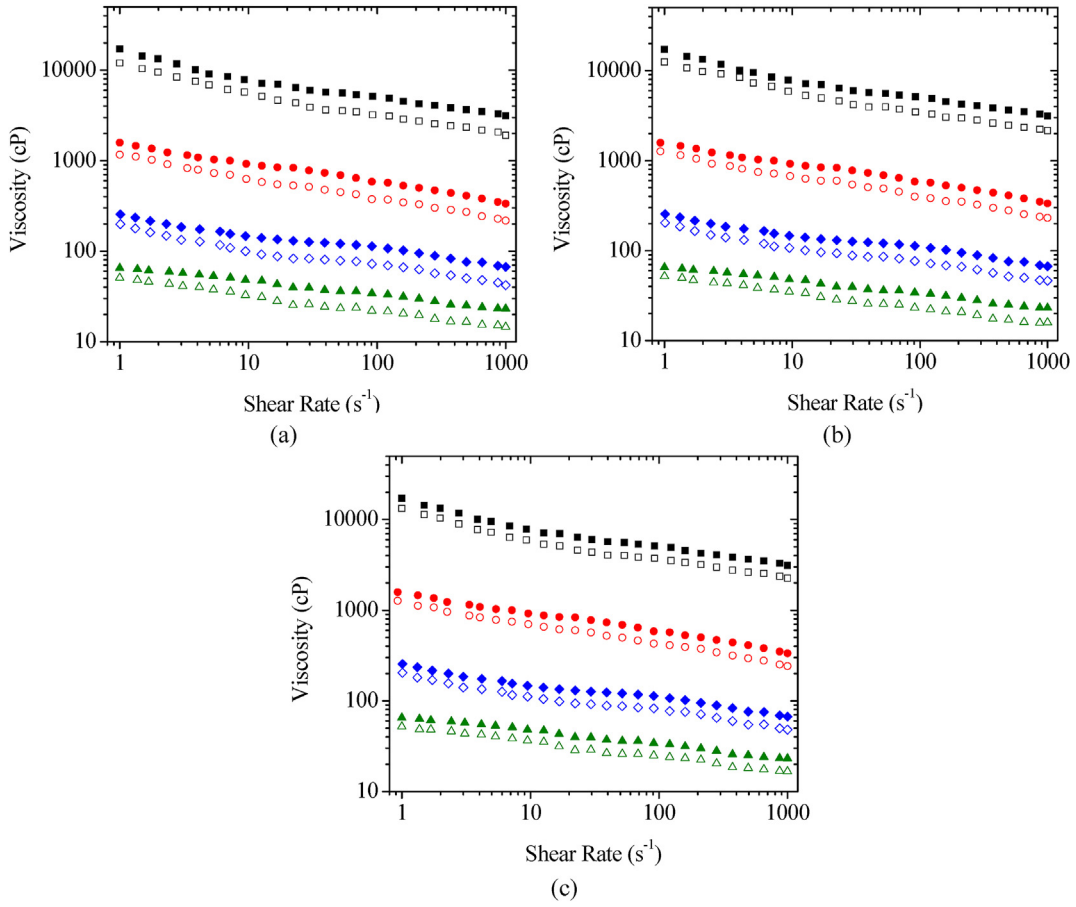

Fig. 2. Shear rheological behavior of the HCO and HCO + ILs at different temperatures in 0.1 MPa. (a) $[Bu_3NH]^+[HSO_4]^-$, (b) $[Pr_3NH]^+[HSO_4]^-$, (c) $[Et_3NH]^+[HSO_4]^-$. ■ HCO (25 °C); □ HCO + IL (25°C); ● HCO (50°C); ○ HCO + IL (50°C); ♦ HCO (75°C); ◊ HCO + IL (75°C); ▲ HCO (100°C); △ HCO + IL (100°C).

species of the ILs as, 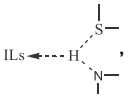 , eventually $[HSO_4]^-$—H interaction will become stronger by weakening the -S—H/-N—H interaction and followed by which it suppressed the possible asphaltene/resin flocculation, it aids to reduce the viscosity of HCO + IL system than the neat HCO. As a result of these processes, the viscosity of the ILs added HCO system is found to be lesser than the neat HCO.

Breaking the structural unit of the asphaltene/resin (hydrogen bonding) molecules into smaller fractions by the addition of ILs could be the main lead for the possible viscosity and density reduction of the HCO [34,38]. The charges present in the broken unit of the HCO's asphaltene/resin units could be surrounded by the corresponding opposite charges from the ILs unit, similar to the simple acid-base or electron donor-acceptors interactions [39]. However, suitable designing of the ILs with longer alkyl chains on the cation and higher charge density on the anion could be employed for successful oil flow in the oil and gas industries. Particularly, this could be most suitable in tackling heavy crude oil depositions, such as pipeline deposition and tank bottom deposition. This study can also be extended for the upstream enhanced oil recovery and downstream oil processing in the refinery section.

3.2. Yield stress measurements

Yield stress (point) is defined as the minimum required stress to deform the materials plastically and below which the material deforms elastically and regains to their original form when releasing the limiting stress, which means the material behaves as a solid below the yield stress (limiting stress) [13,40,41]. To comprehend the flow behavior of any fluid, it is essential to increase applied stress above the yield stress (point) to ensure the fluid flow [37]. Moreover, this section deals with the measurements of the yield stress of the HCO systems with and without ILs as a function of temperature (25, 50, 75, and 100°C) at 0.1 MPa using the Anton Paar Rheometer.

Stress-sweep curves (stress Vs strain) of the neat HCO and HCO + IL samples were generated using the previous viscosity profile of the neat HCO and HCO + IL systems. Fig. 4(a–d) shows the stress-sweep curves (stress Vs strain) relationship of the standard HCO, HCO+$[Et_3NH]^+[HSO_4]^-$, HCO+$[Pr_3NH]^+[HSO_4]^-$, and HCO+$[Bu_3NH]^+[HSO_4]^-$ for four different temperatures (25, 233.15, 75, and 100°C) at 0.1 MPa. No shear flow was noticed until the yield stress was reached. It is also noted that the addition of ILs reduces the yield stresses more significantly irrespective of their temperature and pressure, as shown in Table 4. However, at higher temperatures, the flow of the system sets in a bit early than at lower temperatures, whereas at increasing the pressure, the flow of the system gets delayed than at lower pressure. As seen in Fig. 4 and Table 4, the yield stress of the clean standard HCO was found to be 1.55 Pa at 25°C and it gets dropped to 1.12 Pa when increasing the temperature of the system to 100°C. Thereafter, the addition of 5000 ppm of ILs, $[Et_3NH]^+[HSO_4]^-$, $[Pr_3NH]^+[HSO_4]^-$and $[Bu_3NH]^+[HSO_4]^-$ with standard HCO was evaluated and the yield stress is found to be reduced from 1.55 to 1.05, 1.04, and 1.02 Pa, respectively. However, it is noticed that the addition of ILs with standard HCO reduced the required applied stress to begin the

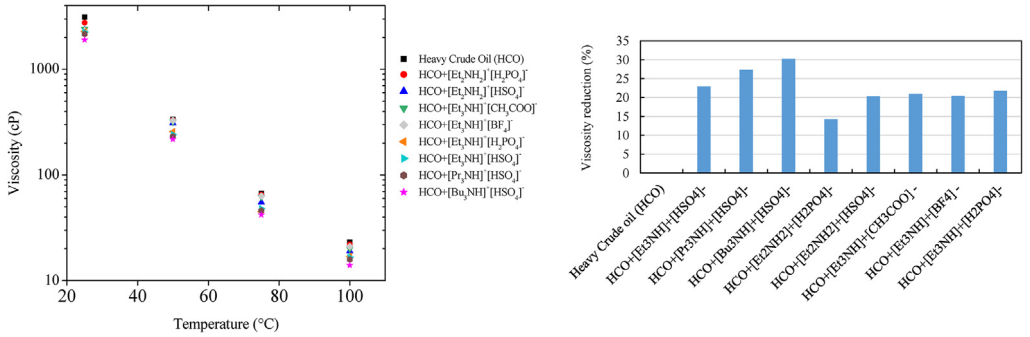

Fig. 3. (a) Effect of ionic liquids (5000 ppm) on the viscosity of HCO (at a shear rate of 1000 s^{-1}) as a function of temperature at 0.1 MPa. (b) Effect of different ionic liquids (5000 ppm) on HCO, and their viscosity reduction efficiency at 25 °C, in 0.1 MPa.

fluid's steady flow. Nevertheless, it is to be understood clearly, that the ILs enhance the ease of fluid flow than the neat HCO system. However, the effect of temperature and pressure on the yield point seems to follow the same trend as we have noticed in the previous section (3.1.1) of shear rheological behavior of the HCO and/or HCO + IL systems.

It is also noticed from Fig. 4(a–d), that a slight variation on the yield stress was experienced for all the systems of HCO and HCO + ILs at the shear rate from 0 to 8-12 s^{-1}. Probably, this could be attributed due to the insufficient magnitude of the applied stress at the region of 0–12 s^{-1}. During this time, the applied stress was not enough to deform the HCO's physical structure, which could have improved the fluids' flow-ability [42,43]. However, when increasing the shear rate of more than 12 s^{-1}, it shows increased flow-ability with a non-linear increase of the yield stress, for both the HCO and HCO + ILs systems. Measuring the yield stress more accurately seems to be the toughest task for these HCO and HCO + ILs systems due to the lower magnitude of the applied stresses below 12 s^{-1}. Moreover, the measured yield stress is found to have uncertainties of 2–4%, even though it has good application values in the oilfield industries.

3.3. Dynamic viscoelastic properties of HCO and HCO + IL solutions

Investigating the viscoelastic properties of the non-Newtonian fluids such as HCO and HCO + ILs mixture is the essential phenomena to understand fluid movement in porous media (reservoirs). Moreover, it is a kind of dynamic testing method, since the measurement is performed during the fluid's movement. The oscillating stress and/or strain was studied for the HCO and HCO + ILs, which leads to measure the viscoelasticity of the fluids under motion. Principally, this dynamic oscillatory test calculates the elasticity when varying the strain and reveals the maximum tolerance of the strain before the sample undergoes shear thinning. Storage or elastic modulus is referred to as G′, which refers to the amount of stress-energy that is stored temporarily during the measurement, and, can be reversed/recovered. Similarly, the Loss or viscous modulus is labeled as G″, is the amount of energy that is required to commence the fluid flow, i.e., the energy is dissipated instead of getting stored, and, moreover, is an irreversible process. However, this viscoelasticity occurrence is the representation of how fluids interact within the sample (HCO) and with ILs, thereby, measuring the physical and structural changes of the HCO sample on ILs addition. Also, the effect of temperature and pressure was also studied in detail.

3.3.1. Standard heavy crude oil

At the beginning of the viscoelastic study, the strain-sweep measurements of the standard HCO sample were performed. Dynamic shear rheological property of storage (G′) and loss modulus (G″) of the standard HCO was studied as a function of temperature and pressure. Fig. 5(a–d), shows the viscoelastic moduli of the strain-sweep measurements of the standard HCO sample at different temperatures (25, 233.15, 75, and 100°C) and pressures (0.1, 2.5, 5 and 10 MPa). It is noticed from Fig. 5a, the measured viscoelastic moduli (strain sweep) of the standard HCO was found to be G' ≈ 11.1 and G" ≈ 7.02 Pa (at the strain around 1.5%) at 25°C, and in 0.1 MPa. It is the indication that the HCO system represents more solid behavior in this condition. Strain dependence of this standard HCO was also monitored from 1 to 100% strain, at the same experimental condition (at 25°C and in 0.1 MPa), wherein the linear viscoelastic region was observed approximately from 1.5 to 20%, thereafter, its G′ decreased gradually, which may be due to relaxation and extrication of HCO's molecules. On the other hand, the measurement of the loss modulus (G″) was found to have a minor drop in the beginning (from 1.5 to 2.5% of the strain), but, further, got maintained to reach the plateau of up to 20% of the stain, and, thereafter, augmented steadily as expected. Overall, Fig. 5a is implicit that the standard HCO exhibits viscoelastic behavior, wherein the major parts of the curve show the elasticity and the rest depict liquid nature at higher strain amplitude. Crossover frequency or the gel-point of this study was identified at around 45% of the applied strain amplitude.

Measurement of the viscoelasticity of the standard HCO at high pressure revealed more of elasticity behavior. As shown in Fig. 5a, the storage modulus of the standard HCO was found to be increased to a larger magnitude as 21.1, 124.3, 145.1, 160.4 Pa (at 1.5% strain) when increasing the system pressure continuously as 2.5, 5, 7.5, and 10 MPa, respectively, at the constant system temperature of 25°C. For the pressure of 2.5 MPa, the storage modulus is found to be almost constant with minor reduction at the end of the strain amplitude, however, the loss modulus was also found to be constant until around 20–30% of the applied strain, thereafter, it tends to steep up and reached the gel-point with the crossover frequency of 95% of the applied strain. For the other studied pressure dependence of 5, 7.5, and 10 MPa, no considerable change in the storage and loss modulus (G′ and G″) was noticed while increasing the applied strain amplitude, and, also, no crossover was observed. Though it is noticed that G′ is always found to be higher than the G″ of the standard HCO at the increased system's pressure of 5, 7.5 and 10 MPa, the constant plateau behavior throughout the applied strain (1–100%) is observed due to more of solid nature of the sample [44]. It is an indication that the applied strain amplitude is not enough to make the structural changes (deformation) of the standard HCO at this high pressure as compared to 0.1 MPa since the sample behaves more like solid. A similar pressure dependence study was performed with an increase in temperature and presented in Fig. 5b, c, and 5d.

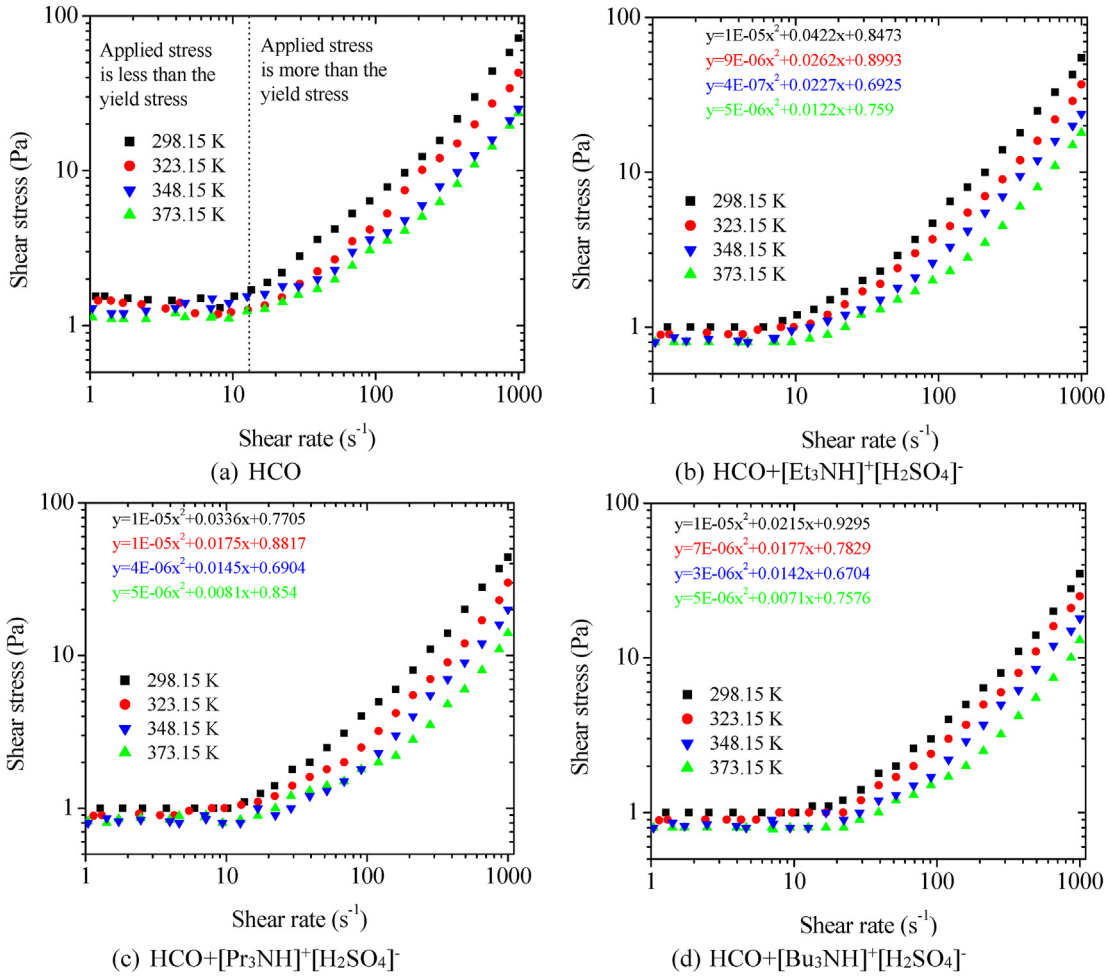

Fig. 4. Plots of shear stress vs shear rate for standard (a) HCO, (b) HCO+$[Et_3NH]^+[H_2SO_4]^-$, (c) HCO+$[Pr_3NH]^+[H_2SO_4]^-$ and (d) HCO+$[Bu_3NH]^+[H_2SO_4]^-$ sample as a function of temperature (25–100°C) at 0.1 MPa.

Table 4
Yield stress values of the various systems of the HCO, HCO + ILs at four different temperatures in 0.1 MPa pressure.

Systems	Temperature (°C)	Yield stress (Pa)
HCO	25	1.55
	50	1.45
	75	1.22
	100	1.12
HCO+$[Et_3NH]^+[HSO_4]^-$	25	1.05
	50	0.92
	75	0.88
	100	0.86
HCO+$[Pr_3NH]^+[HSO_4]^-$	25	1.04
	50	0.89
	75	0.85
	100	0.82
HCO+$[Bu_3NH]^+[HSO_4]^-$	25	1.02
	50	0.88
	75	0.82
	100	0.80

In addition to the pressure effect, the temperature dependence of the standard HCO was also studied using the same strain sweep analysis and presented in Fig. 5a–d. As mentioned in the experimental section, four different temperatures (25, 50, 75, and 100°C) were studied for this analysis. For each temperature of 25, 50, 75, and 100°C, the pressure dependence was also studied and presented in Fig. 5a, b, 5c, and 5c respectively. An increase in temperature tends to reduce both the G′ and G″ more significantly in magnitude irrespective of the system's pressure. At 50°C and 0.1 MPa, it was observed that their crossover frequency (G' ≈ G″) was around 9.1% of the applied strain amplitude (see Fig. 5b). For 2.5 MPa pressure of the same system, the crossover frequency at around 40% was observed since higher the pressure, higher is the tendency of the material to become more like a solid. For the other studied pressures, 2.5, 5, 7.5, and 10 MPa, there is no crossover occurrence, due to their increased solid behavior. For the increased system's temperature to 75 and 100°C, no crossover frequency was witnessed and with increased loss modulus than storage modulus at 0.1 MPa, the system behaved more of liquid-like material (G″ is higher than G′). However, when increasing the pressure of the system at 75°C, a crossover at around 10, 10.5, 11% of strain was noted for the pressures 5, 7.5 and 10 MPa, respectively. For the temperature of 100°C, the system behaved completely liquid-like (G″ is much higher than G′ values) irrespective of the pressure.

Additionally, frequency-sweep experiments were also carried out for the same system of standard HCO, as a function of temperature and pressure to support the strain-sweep experiments. Frequency-sweep analysis of the standard HCO was performed, at the LVE region of 1.5% of strain amplitude, (this linear viscoelastic region was evaluated using the strain-sweep), as a function of temperature (273.15–100°C) and pressure (0.1–10 MPa). Fig. 6a–d shows the measured frequency-sweep viscoelasticity of the standard HCO at four different temperatures and five various pressures.

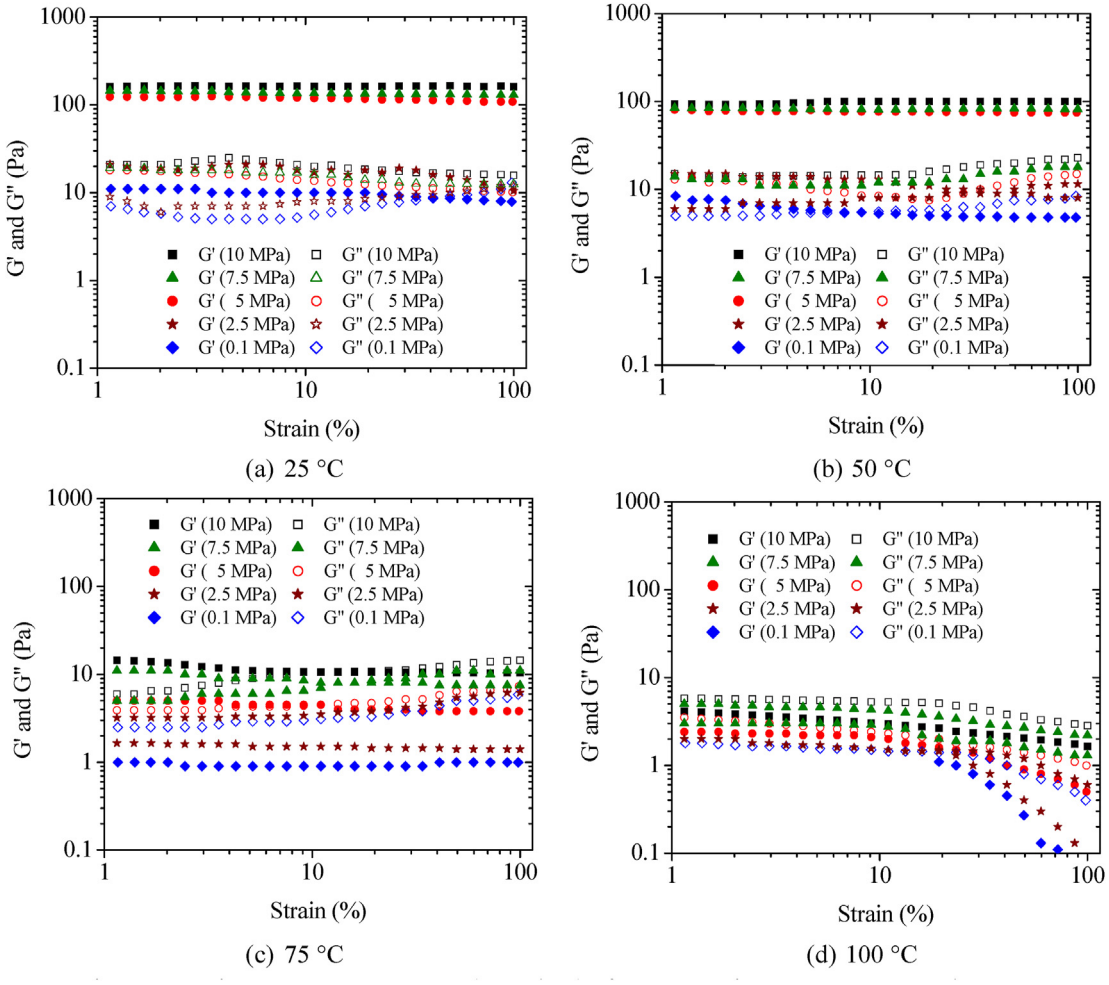

Fig. 5. Strain-sweep measurements (G′ and G″) of HCO at various temperatures and pressure of 0.1, 2.5, 5, 7.5, and 10 MPa. G' (solid symbols) and G" (open symbols).

Fig. 6(a), shows the pressure dependence (0.1–10 MPa) of the standard HCO's viscoelasticity test (frequency-sweep), at the temperature of 25°C. The crossover frequency has been noticed for the lower pressure of system (0.1 MPa), at around 11.2 rad s^{-1}. This is in line with the strain-sweep experiments. Also, their storage modulus was found to be higher in value than the loss modulus at the beginning of the experiments, however, it crossed at 11.2 rad·s^{-1}, then the loss modulus took lead due to the higher applied frequency. When increasing the pressure to 2.5 MPa, the crossover was found to move towards the right side, with the higher applied frequency of 19.3 rad·s^{-1}. Similarly, when increasing the pressure further to 5, 7.5 and 10 MPa, it turned to a situation of no crossover point with a higher value of storage modulus (G′) than the loss modulus (G″), which confirmed the characteristic behavior of gel. However, on increasing the applied frequency (>50 rad·s^{-1}), the lowering of their storage modulus was seen. It means that the system behaves as viscoelastic at lower pressure and seems to behave as a gel at increased pressures (5, 7.5 and 10 MPa).

Besides, temperature dependence (25–100°C) studies were also carried out for the same system with five different pressures (0.1–10 MPa) and it is displayed in Fig. 6(a)-(d). The crossover at 3.5 rad·s^{-1} was observed for the system of 0.1 MPa at 50°C (Fig. 6b), which is slightly shorter than the same system at a lower temperature (25 °C) (11.2 rad·s^{-1}) (see Fig. 6(a)). At the same temperature (50°C), with an increase in pressure of 2.5 MPa, the system showed the crossover point at 19.08 rad·s^{-1}, which is very close to their previous temperature (25°C) value, though, slightly lower as expected. For the higher pressures (5, 7.5 and 10 MPa), the system followed a similar trend as in Fig. 6(a). When increasing the system's pressure from 0.1 to 10 MPa in Fig. 6b, their storage modulus increases from 8.1 Pa (0.1 MPa) to 142 Pa (10 MPa), which means the standard HCO is slowly transforming into a gel-like material, and, eventually, getting solidified. Further increase of the temperature of the system to 75 and 100°C, for 0.1 MPa, showed no crossover point, and the loss modulus interaction had already taken a lead over the storage modulus even at lower applied frequency. However, the increase of the system's pressure (Fig. 6c and d), causes an increase in the storage modulus followed by which occurs the crossover point. Hence, the observed crossover point is to be noted as 2.9 and 8.2 rad·s^{-1}, for the pressure of 7.5 and 10 MPa, respectively, at 75. Similarly, for the temperature of 100°C, their crossover points were observed as 3.25 and 3.5 rad·s^{-1}, for the corresponding pressures of 7.5 and 10 MPa. Overall, it can be noted from Fig. 6c and d, the material behaves more like a viscous substance (increased temperature), due to their lower relaxation and extrication (molecules disconnection), which slowly turns to viscoelastic when increasing system's pressure (7.5 and 10 MPa). On comparing all the four temperatures from 25 to 100°C (Fig. 6a–d), it can be understood that on increasing the system's temperature, their storage modulus value is gradually decreasing and their loss modulus steeply increases. The reverse is evident upon increasing the system's pressure.

As a summary, at higher temperature's (75 and 100°C), and at lower frequencies the system behaves more of viscoelastic by the appearance of both G′ and G″ and when increasing the system's frequency more than 5–8 rad·s^{-1}, it acts like a viscous fluid due to domination of increased loss modulus (G″). Fig. 7, depicts the temperature dependence (25–100°C) of the HCO's viscoelasticity over various pressures (0.1–10 MPa). It is noticed from Fig. 7 that the appearance of viscoelasticity (crossover point) is observed to be at a lower temperature (320–340 K) for the lower's system pressure and which is increased to 360–370 K when increasing the system's pressure to 10 MPa. The changes of the elastic property to viscous (solid-like to liquid-like) nature of the HCO occurred (where G' ≈ G″), at around 331, 337, 357, 365 and 370 K, for the various pressures of 0.1, 2.5, 5, 7.5 and 10 MPa, correspondingly (see Fig. 7). Mostly at a lower temperature, the HCO behaved as elastic (more of storage modulus than loss modulus), and when increasing the temperature, it turned viscous (more of loss modulus than storage modulus) irrespective of the pressure. It occurs due to the viscosity/extrication reduction of the HCO systems over temperature. Moreover, the frequency-sweep experiments are in line with the strain-sweep experiments and confirming the effect of temperature and pressure on the viscoelasticity.

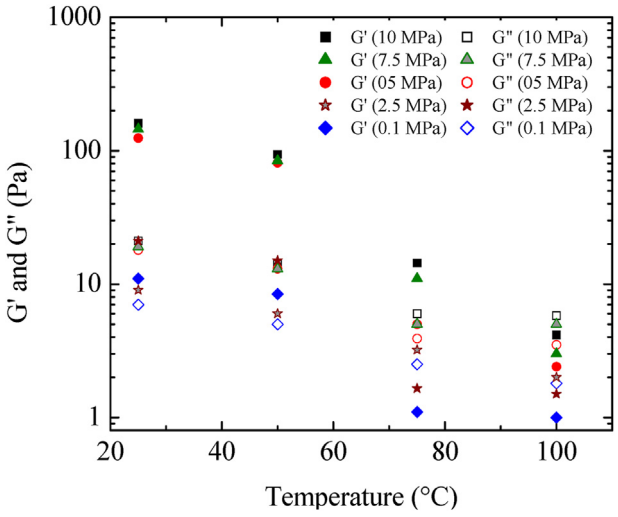

Fig. 7. Effect of temperature (25–100°C) on G′ (solid symbols) and G″ (open symbols) of the standard HCO systems at the pressures of 0.1, 2.5, 5, 7.5 and 10 MPa.

3.3.2. *Effect of ILs on the dynamic viscoelasticity of heavy crude oil*

Dynamic viscoelasticity (G′ and G″) of the HCO with the addition of different alkyl ammonium-based ionic liquids were also studied for both the strain-sweep and frequency-sweep analysis. This was intended to understand the effect of ionic liquids on the shear rheological behavior of the HCO over the ILs addition. This would help us understand the flow property of the HCO fluids with and without ILs at high temperature and high salinity. Fig. 8a–h, shows the effect of eight different alkyl ammonium ILs (5000 ppm or 0.5 wt %), on the standard HCO's shear rheological viscoelasticity

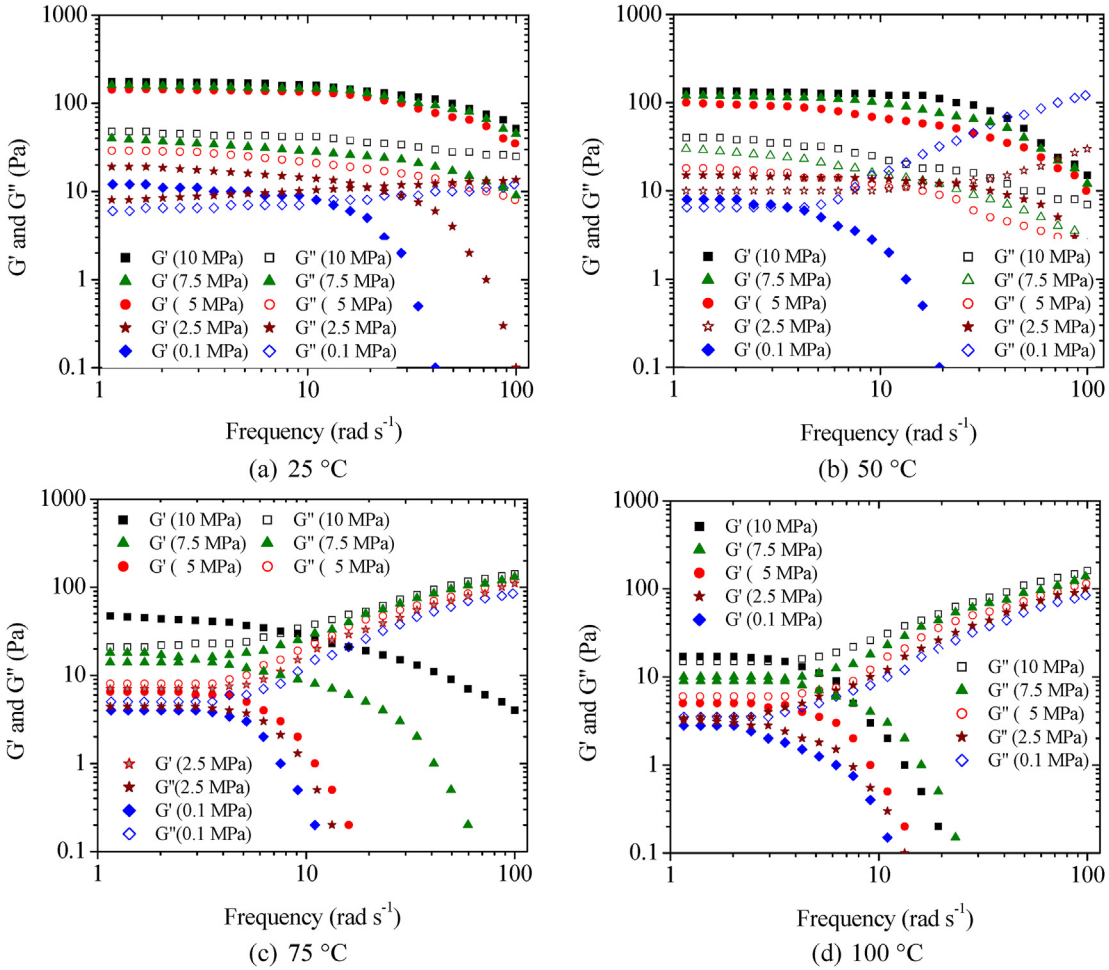

Fig. 6. Frequency-sweep measurements (G′ and G″) of HCO at various temperatures and pressure of 0.1, 2.5, 5, 7.5, and 10 MPa. G' (solid symbols) and G" (open symbols).

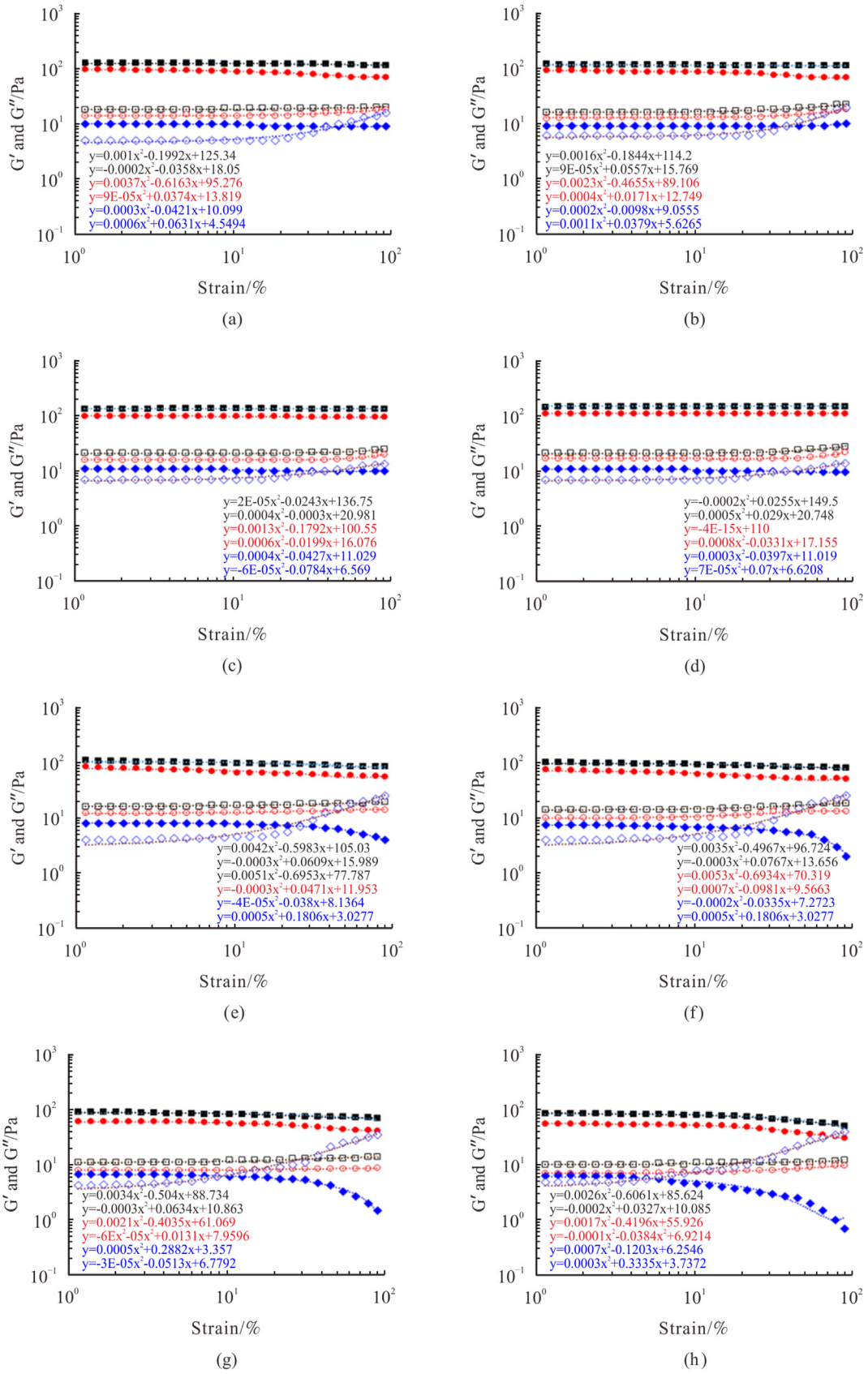

Fig. 8. Strain-sweep measurements (G′ and G″) of HCO + ILs for eight different ILs, in various pressures (◆ G′ and ◇ G″ at 0.1 MPa; ○ G′ and ● G″ at 5 MPa; □ G′ and ■ G″ at 10 MPa) at 25°C.

(strain dependence) at 25°C and at five various pressures (presented only three pressures (0.1, 5 and 10 MPa) for the better clarity). It is noticed that the addition of ILs, $[Et_2NH_2]^+[H_2PO_4]^-$, $[Et_2NH_2]^+[HSO_4]^-$, $[Et_3NH]^+[CH_3COO]^-$, $[Et_3NH]^+[BF_4]^-$, $[Et_3NH]^+[H_2PO_4]^-$, $[Et_3NH]^+[HSO_4]^-$, $[Pr_3NH]^+[HSO_4]^-$ and $[Bu_3NH]^+[HSO_4]^-$ to the HCO reveals a clear reduction of the crossover point (viscoelasticity) to 42.7, 41.1, 41.46, 40.89, 28.19, 23.64, 9.4, and 5.3% of the strain amplitude correspondingly (see Fig. 8a–h) for 0.1 MPa pressure. However, the observed viscoelastic crossover points of the HCO + IL mixtures are found to be much lesser than the standard HCO's crossover point (45% of the strain amplitude, see Fig. 5a). Irrespectively, the addition of any ILs reduced the material's storage modulus (solid-like behavior (G′)) more significantly than the standard HCO's storage modulus, while it increased the fluid's loss modulus (liquid-like behavior, G″) noticeably. However, when increasing the system's pressure to 5 and 10 MPa from 0.1 MPa, their storage modulus is also increased a bit with no crossover point, due to the domination of G′, as expected, though, their values are much lesser when compared to the standard HCO's storage modulus value at the corresponding experimental pressure of 5 and 10 MPa. It is an indication that IL has the capability to reduce the fluid's viscosity and viscoelasticity by increasing the loss modulus (G″) substantially to improve the fluid's flow-ability to a greater extent. The measured storage (G′) and loss (G″) moduli of both the HCO and HCO + ILs samples are summarized in Table 5. It depicts the ILs containing lengthier alkyl chain, such as $[Bu_3NH]^+[HSO_4]^-$ and $[Pr_3NH]^+[HSO_4]^-$ which are found to be more efficient on improving flow-ability by increasing G′ and reducing G″ simultaneously.

In the same way, the frequency-sweep experiments of the HCO + ILs were also studied as a function of temperature and pressure. Fig. 9a–h shows the effect of eight different alkyl ammonium ILs on the HCO's frequency-sweep test at 25 °C in three various pressures of 0.1, 5, and 10 MPa. For the HCO + ILs, the frequency-sweep test shows the crossover frequency only at the lower pressure of 0.1 MPa, similar to the strain-sweep analysis. The observed crossover frequency of the HCO + ILs are 10.15, 10.1, 10.2, 10.1, 10.05, 9.95, 9.9, and 8.2 rad s^{-1} for the addition of ILs, $[Et_2NH_2]^+[H_2PO_4]^-$, $[Et_2NH_2]^+[HSO_4]^-$, $[Et_3NH]^+[CH_3COO]^-$, $[Et_3NH]^+[BF_4]^-$, $[Et_3NH]^+[H_2PO_4]^-$, $[Et_3NH]^+[HSO_4]^-$, $[Pr_3NH]^+[HSO_4]^-$ and $[Bu_3NH]^+[HSO_4]^-$, respectively, at 0.1 MPa. As discussed before, all these observed crossover frequencies are relatively lesser than the neat standard HCO's crossover frequency (11.2 rad s^{-1}) at the same experimental condition. However, when increasing the system's pressure to 5 and 10 MPa, it leads to dominating the storage modulus (G′) more substantially with no crossover frequency for the complete region of the frequency sweep. Hence, it is understood that the addition of each and every IL, reduces the storage modulus and crossover frequency more substantially than the standard HCO sample at the same experimental condition.

3.4. Microscopic characterization

In addition to the rheological studies, a simple microscopic investigation of the HCO + IL emulsions (1:0.1 ratio of HCO:IL) was also studied to understand the ILs efficiency on the HCO at 25°C. In the beginning, the standard HCO was analyzed under an inverted microscope (Leica, Germany) using 100× magnification and is presented in Fig. 10a and Fig. 10b–d shows the microscopic images of the addition of three best different ILs, $[Bu_3NH]^+[HSO_4]^-$, $[Pr_3NH]^+[HSO_4]^-$, and $[Et_3NH]^+[HSO_4]^-$ to HCO. The neat HCO sample (see Fig. 10a) contains more of irregular (non-uniform) shapes of emulsion. It shows highly irregular large moieties of the flocculated unit of the HCO sample, which is mainly the contribution of polar fractions of the HCO sample, such as asphaltene, resins, and complex aromatics [27,28]. With the addition of ILs, the observed large flocculated fraction of the HCO (heavier fraction of the HCO), was found to be fragmented into smaller spheres (see Fig. 10b–d), which enable the ease of fluid flow. As noticed in the previous sections (3.1, 3.3), when analyzing all the eight various alkyl ammonium ILs, the ILs with lengthier alkyl chain length, such as $[Bu_3NH]^+[HSO_4]^-$, $[Pr_3NH]^+[HSO_4]^-$, and $[Et_3NH]^+[HSO_4]^-$ (see Fig. 10b–d) shows better efficiency on breaking the fluids asphaltene/resin/aromatics unit than the other studied ILs (Fig. 10d). This is in line with the rheological studies of different ILs on HCO. As discussed before, this could be due to the better hydrophobicity interactions of the longer chain containing ILs with the HCO [17,29,30]. Also, it is expected that the added ILs could have reduced the intramolecular interaction of the HCO, such as reduction of asphaltenes precipitation and hydrogen bond reduction, etc. Asphaltenes/resins being large molecular weight heavier fractions, get aggregated or precipitated by the intermolecular electrostatic interactions which are mainly responsible for higher viscosity of the HCO. Asphaltene and resins are the main polar components of the HCO and are largely constituted with polar substituents like –OH, –NH, and –SH moieties. Basically, they tend to form hydrogen bonds between each other (–OH, –NH and –SH) like,  , wherein once it gets exposed to ILs, the anionic portion of the ILs could reduce this interaction substantially, by attracting the hydrogen towards the ILs, 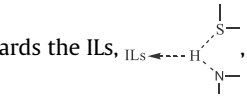 , which means

Table 5
Viscoelastic Properties of HCO and HCO + ILs, as a function of different temperatures and pressures.

System	Strain-sweep frequency (rad.s^{-1})	Strain amplitude (%)	T (K)	Dynamic moduli (Pa)					
				0.1 MPa		5 MPa		10 MPa	
				G′	G″	G′	G″	G′	G″
Heavy crude oil (HCO)	10	1.5	25	11.1	7.02	124.3	18.06	160.4	21.3
	10	1.5	50	8.44	5.08	81.1	13.05	994.4	15.1
	10	1.5	75	0.96	2.59	5.05	3.96	14.41	6.01
	10	1.5	100	–	1.83	2.45	3.56	4.19	5.87
$[Et_2NH_2]^+[H_2PO_4]^-$	10	1.5	25	10	5	95	14	125	18
$[Et_2NH_2]^+[HSO_4]^-$	10	1.5	25	9	6	90	12	118	16
$[Et_3NH]^+$ $[CH_3COO]^-$	10	1.5	25	11	7	100	16	135	21
$[Et_3NH]^+[BF_4]^-$	10	1.5	25	11	7	110	17	145	21
$[Et_3NH]^+[H_2PO_4]^-$	10	1.5	25	8	4	84	12	109	16
$[Et_3NH]^+[HSO_4]^-$	10	1.5	25	6.7	4.3	105	23	140	35
$[Pr_3NH]^+[HSO_4]^-$	10	1.5	25	6.7	4.2	60	8	90	11
$[Bu_3NH]^+[HSO_4]^-$	10	1.5	25	6.3	4.8	55	7	85	10

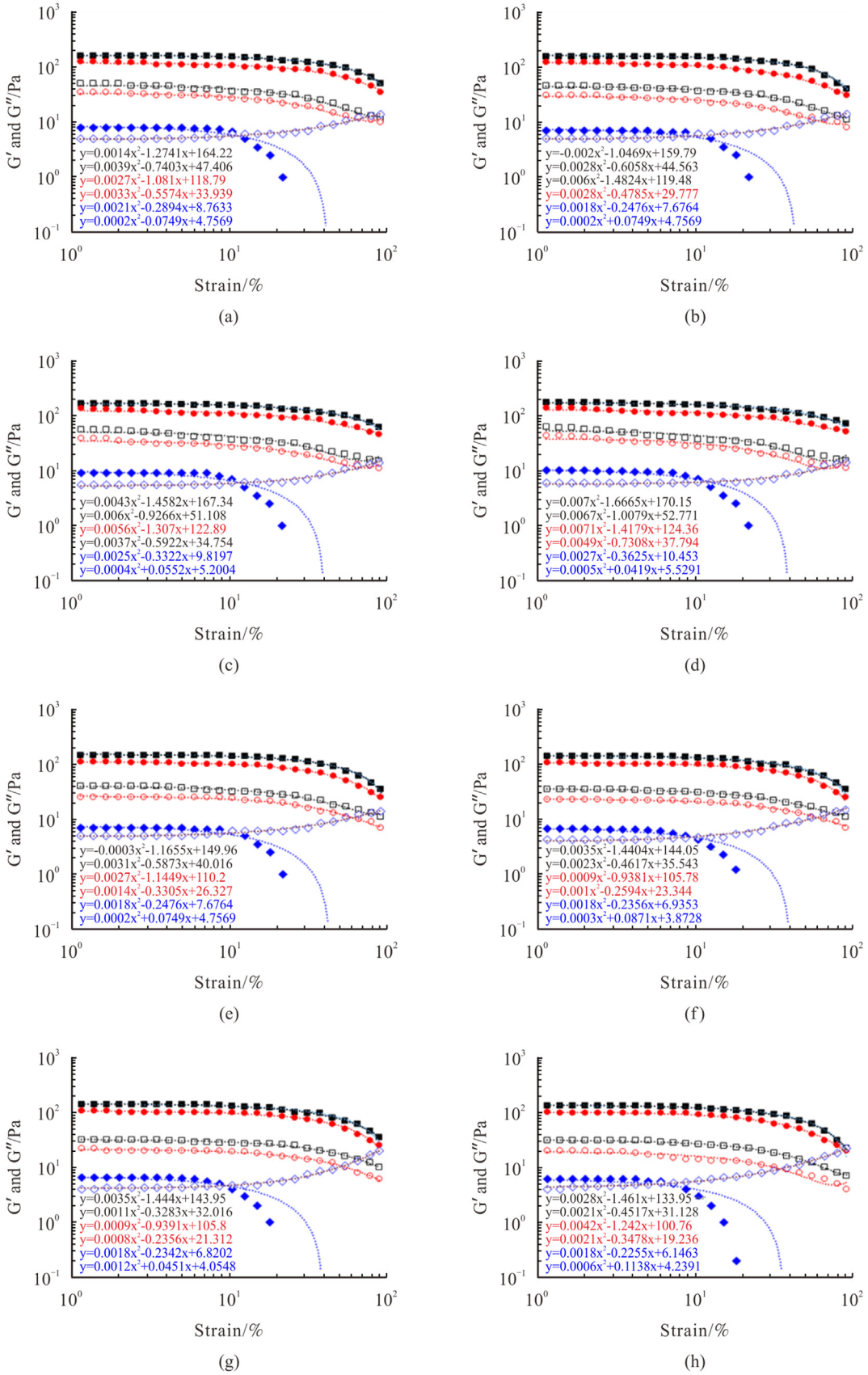

Fig. 9. Frequency -sweep measurements (G′ and G″) of HCO + ILs for eight various ILs, in various pressures (◆ G′ and ◇ G″ at 0.1 MPa; ○ G′ and ● G″ at 5 MPa; □ G′ and ■ G″ at 10 MPa) at 25 °C.

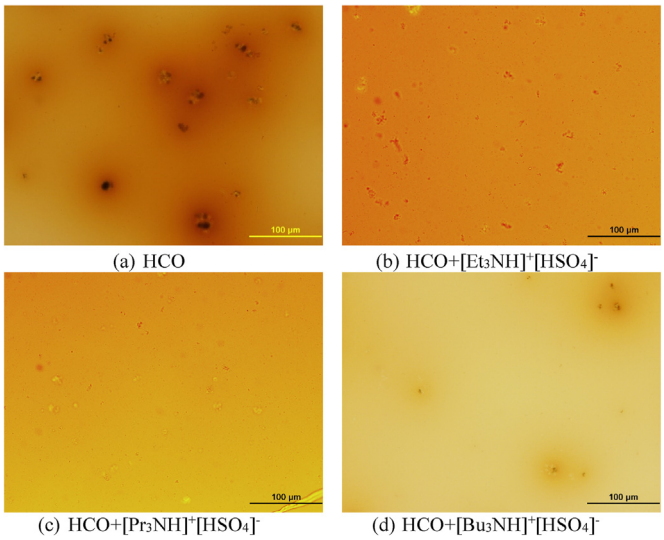

Fig. 10. Surface morphology (Microscopic images) of the standard HCO and HCO + IL systems at 25 °C.

ammonium-based ILs are found to be more eco-efficient (lesser toxic) than any aromatic core containing ILs, such as imidazolium, pyridinium, thiazolium, etc. Also, the IL which has the shorter chain length showed lesser toxicity than lengthier chain ionic liquids. In addition to this, the anions such as Br^-, Cl^-, NO_3^-, HSO_4^-, and CH_3COO^- are witnessed as eco-efficient [46–49]. Hence, it is to be believed that these inexpensive alkyl ammonium ILs could be a better option to enhance the oil flow since it is extremely cheaper and lesser toxic than the other conventional ionic liquids.

4. Conclusions

This study reveals the effect of *eight* different alkyl ammonium ILs ($[Et_2NH_2]^+[H_2PO_4]^-$, $[Et_2NH_2]^+[HSO_4]^-$, $[Et_3NH]^+[CH_3COO]^-$, $[Et_3NH]^+[BF_4]^-$, $[Et_3NH]^+[H_2PO_4]^-$, $[Et_3NH]^+[HSO_4]^-$, $[Pr_3NH]^+[HSO_4]^-$ and $[Bu_3NH]^+[HSO_4]^-$) on the rheological behavior of the HCO at various experimental conditions. It was witnessed that the addition of ILs to HCO reduces the oil viscosity more substantially, up to 31.5% (at 25°C, 0.1 MPa), from their original viscosity. It also reduces the yield stresses of HCO to around 15–30%, irrespective of any temperature (25–100°C) and pressure (0.1–10 MPa). Visco-elastic measurements of the HCO system showed a substantial

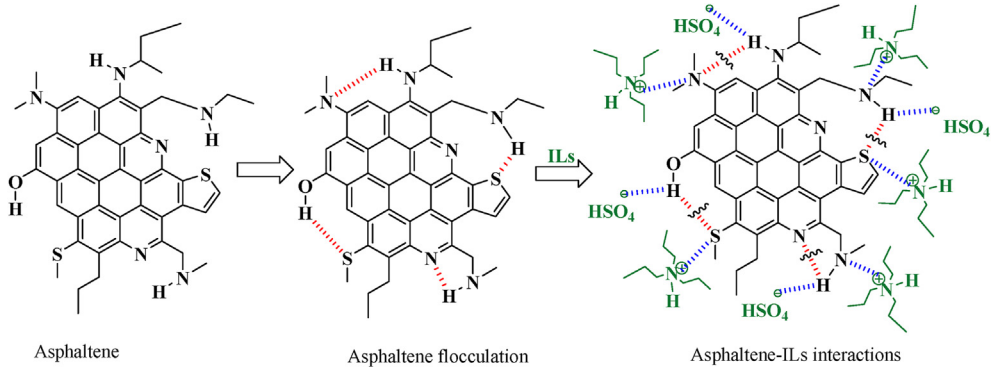

Fig. 11. Proposed mechanism showing the interaction of the ionic liquids with the asphaltene/resin/aromatic components of the heavy crude oil. Black colored structure represents the asphaltene/resins/aromatics and green colored structure denotes the ILs.

the asphaltene and resins get diffused with ILs, followed by fragmentation of asphaltene cage structure into single or smaller fractions, which will reduce the HCO's viscosity. To support this phenomenon, another possibility could be the positive charge of the ILs which could have a weaker electrostatic interaction with the lone pair of the heteroatoms of asphaltene/resin. Once the ILs interact with asphaltenes, the reversibility of the asphaltene precipitation could be suppressed by placing the lengthier chains of ILs as a steric hindrance which is more enough to cease the reversibility. Probably, this could be the reason behind the greater efficiency of lengthier alkyl chain over the shorter chain ILs. Fig. 11 demonstrates graphically the proposed mechanism to reduce oil viscosity. Moreover, the caged structure of the HCO gets solvated enough with ILs to enhance oil flow-ability. This convincingly better efficiency of the lengthier alkyl chain containing ILs towards better viscosity reduction can further be supported by the studies of Jian et al. (2013), where the author had studied the molecular simulation of the alkyl chain length on the larger hydrocarbon and observed similar trends [45]. Though ionic liquids are considered green solvents, this is in fact merely based on their physicochemical properties of the ionic fluids, such as high level thermal and chemical stability and excellent solvation tendency. However, the recent toxicological studies of the ionic liquids with various microorganisms revealed that the non-aromatic IL, such as alkyl reduction in the crossover frequency (~3.45 rad · s^{-1}) by the ILs addition. Overall, the ILs are convincing in all aspects of rheological improvement (viscosity, yield stress, strain sweep, and frequency sweep crossover points). Furthermore, optical microscopic images showed the reduction of oil's aggregation with ILs addition, which is further supporting the rheological studies. However, in all the *eight* studied ILs, the one with the lengthier chain length ($[Bu_3NH]^+[HSO_4]^-$) showed better efficiency than other ILs. This study indicates that the ILs have the capability to increase the oil's flow capacity by reducing their viscosity, even at high temperature and high pressure.

Acknowledgment

The author would like to thank the Center for Integrative Petroleum Research (CIPR), College of Petroleum Engineering & Geosciences, King Fahd University of Petroleum & Minerals for the laboratory support throughout this research work.

Appendix A. Supplementary data

Supplementary data to this article can be found online at https://doi.org/10.1016/j.petlm.2021.06.002.

References

[1] A. Shah, R. Fishwick, J. Wood, G. Leeke, S. Rigby, M. Greaves, A review of novel techniques for heavy oil and bitumen extraction and upgrading, Energy Environ. Sci. 3 (2010) 700, https://doi.org/10.1039/b918960b.

[2] S. Sakthivel, A. Adebayo, M.Y. Kanj, Experimental evaluation of carbon dots stabilized foam for enhanced oil recovery, Energy Fuel. 33 (2019) 9629–9643, https://doi.org/10.1021/acs.energyfuels.9b02235.

[3] A. Saniere, I. Hénaut, J.F. Argillier, Pipeline transportation of heavy oils, a strategic, economic and technological challenge, Oil Gas Sci. Technol. 59 (2004) 455–466, https://doi.org/10.2516/ogst:2004031.

[4] D. Subramanian, K. Wu, A. Firoozabadi, Ionic liquids as viscosity modifiers for heavy and extra-heavy crude oils, Fuel 143 (2015) 519–526, https://doi.org/10.1016/J.FUEL.2014.11.051.

[5] M.T. Ghannam, S.W. Hasan, B. Abu-Jdayil, N. Esmail, Rheological properties of heavy & light crude oil mixtures for improving flowability, J. Petrol. Sci. Eng. 81 (2012) 122–128, https://doi.org/10.1016/J.PETROL.2011.12.024.

[6] S. Shaban, S. Dessouky, A.E.F. Badawi, A. El Sabagh, A. Zahran, M. Mousa, Upgrading and viscosity reduction of heavy oil by catalytic ionic liquid, Energy Fuel. 28 (2014) 6545–6553, https://doi.org/10.1021/ef500993d.

[7] B.M. Yaghi, A. Al-Bemani, Heavy crude oil viscosity reduction for pipeline transportation, Energy Sources 24 (2002) 93–102, https://doi.org/10.1080/00908310252774417.

[8] M. Meriem-Benziane, S.A. Abdul-Wahab, M. Benaicha, M. Belhadri, Investigating the rheological properties of light crude oil and the characteristics of its emulsions in order to improve pipeline flow, Fuel 95 (2012) 97–107, https://doi.org/10.1016/J.FUEL.2011.10.007.

[9] O.A. Alomair, A.S. Almusallam, Heavy crude oil viscosity reduction and the impact of asphaltene precipitation, Energy Fuel. 27 (2013) 7267–7276, https://doi.org/10.1021/ef4015636.

[10] J. Jing, J. Tan, H. Hu, J. Sun, P. Jing, Rheological and emulsification behavior of Xinjiang heavy oil and model oils, Open Fuel Energy Sci. J. 9 (2016) 1–10, https://doi.org/10.2174/1876973X01609010001.

[11] Y. Al-Roomi, R. George, A. Elgibaly, A. Elkamel, Use of a novel surfactant for improving the transportability/transportation of heavy/viscous crude oils, J. Petrol. Sci. Eng. 42 (2004) 235–243, https://doi.org/10.1016/J.PETROL.2003.12.014.

[12] H.P. Soni, Kiranbala, D.P. Bharambe, Performance-based designing of wax crystal growth inhibitors, Energy Fuel. 22 (2008) 3930–3938, https://doi.org/10.1021/ef8002763.

[13] S.W. Hasan, M.T. Ghannam, N. Esmail, Heavy crude oil viscosity reduction and rheology for pipeline transportation, Fuel 89 (2010) 1095–1100, https://doi.org/10.1016/J.FUEL.2009.12.021.

[14] N. Sakthipriya, M. Doble, J.S. Sangwai, Biosurfactant from Pseudomonas species with waxes as carbon source – their production, modeling and properties, J. Ind. Eng. Chem. 31 (2015) 100–111, https://doi.org/10.1016/J.JIEC.2015.06.013.

[15] T. Welton, Room-Temperature Ionic Liquids. Solvents for Synthesis and Catalysis, Chem. Rev. 99 (8) (1999) 2071–2084, https://doi.org/10.1021/CR980032T.

[16] N.V. Plechkova, K.R. Seddon, Applications of ionic liquids in the chemical industry, Chem. Soc. Rev. 37 (2008) 123–150, https://doi.org/10.1039/B006677J.

[17] S. Sakthivel, P.K. Chhotaray, S. Velusamy, R.L. Gardas, J.S. Sangwai, Synergistic effect of lactam, ammonium and hydroxyl ammonium based ionic liquids with and without NaCl on the surface phenomena of crude oil/water system, Fluid Phase Equil. 398 (2015) 80–97, https://doi.org/10.1016/J.FLUID.2015.04.011.

[18] S. Sakthivel, R.L. Gardas, J.S. Sangwai, Effect of alkyl ammonium ionic liquids on the interfacial tension of the crude oil–water system and their use for the enhanced oil recovery using ionic liquid-polymer flooding, Energy Fuel. 30 (2016) 2514–2523, https://doi.org/10.1021/acs.energyfuels.5b03014.

[19] S. Velusamy, S. Sakthivel, L. Neelakantan, J.S. Sangwai, Imidazolium-based ionic liquids as an anticorrosive agent for completion fluid design, J. Earth Sci. 28 (2017) 949–961, https://doi.org/10.1007/s12583-017-0780-2.

[20] S. Velusamy, S. Sakthivel, R.L. Gardas, J.S. Sangwai, Substantial enhancement of heavy crude oil dissolution in low waxy crude oil in the presence of ionic liquid, Ind. Eng. Chem. Res. 54 (2015) 7999–8009, https://doi.org/10.1021/acs.iecr.5b01337.

[21] P. Williams, A. Lupinsky, P. Painter, Recovery of bitumen from low-grade oil sands using ionic liquids, Energy Fuel. 24 (2010) 2172–2173, https://doi.org/10.1021/ef901384s.

[22] P. Painter, P. Williams, A. Lupinsky, Recovery of bitumen from Utah tar sands using ionic liquids, Energy Fuel. 24 (2010) 5081–5088, https://doi.org/10.1021/ef100765u.

[23] X. Li, W. Sun, G. Wu, L. He, H. Li, H. Sui, Ionic liquid enhanced solvent extraction for bitumen recovery from oil sands, Energy Fuel. 25 (2011) 5224–5231, https://doi.org/10.1021/ef2010942.

[24] C.G. Hogshead, E. Manias, P. Williams, A. Lupinsky, P. Painter, Studies of Bitumen–Silica and Oil–Silica interactions in ionic liquids, Energy Fuel. 25 (2011) 293–299, https://doi.org/10.1021/ef101404k.

[25] H. Fan, Z. Li, T. Liang, Experimental study on using ionic liquids to upgrade heavy oil, J. Fuel Chem. Technol. 35 (2007) 32–35, https://doi.org/10.1016/S1872-5813(07)60009-7.

[26] S. Sakthivel, R.L. Gardas, J.S. Sangwai, Spectroscopic investigations to understand the enhanced dissolution of heavy crude oil in the presence of lactam, alkyl ammonium and hydroxyl ammonium based ionic liquids, J. Mol. Liq. 221 (2016) 323–332, https://doi.org/10.1016/J.MOLLIQ.2016.05.062.

[27] S. Sakthivel, S. Velusamy, R.L. Gardas, J.S. Sangwai, Eco-efficient and green method for the enhanced dissolution of aromatic crude oil sludge using ionic liquids, RSC Adv. 4 (2014) 31007–31018, https://doi.org/10.1039/C4RA03425B.

[28] S. Sakthivel, S. Velusamy, R.L. Gardas, J.S. Sangwai, Experimental investigation on the effect of aliphatic ionic liquids on the solubility of heavy crude oil using UV–visible, fourier transform-infrared, and 13 C NMR spectroscopy, Energy Fuel. 28 (2014) 6151–6162, https://doi.org/10.1021/ef501086v.

[29] S. Sakthivel, S. Velusamy, R.L. Gardas, J.S. Sangwai, Use of aromatic ionic liquids in the reduction of surface phenomena of crude oil–water system and their synergism with brine, Ind. Eng. Chem. Res. 54 (2015) 968–978, https://doi.org/10.1021/ie504331k.

[30] S. Sakthivel, S. Velusamy, R.L. Gardas, J.S. Sangwai, Adsorption of aliphatic ionic liquids at low waxy crude oil–water interfaces and the effect of brine, Colloids Surfaces A Physicochem. Eng. Asp. 468 (2015) 62–75, https://doi.org/10.1016/J.COLSURFA.2014.12.010.

[31] S. Sakthivel, S. Velusamy, V.C. Nair, T. Sharma, J.S. Sangwai, Interfacial tension of crude oil-water system with imidazolium and lactam-based ionic liquids and their evaluation for enhanced oil recovery under high saline environment, Fuel 191 (2017) 239–250, https://doi.org/10.1016/j.fuel.2016.11.064.

[32] S. Velusamy, S. Sakthivel, J.S. Sangwai, Effects of imidazolium-based ionic liquids on the rheological behavior of heavy crude oil under high-pressure and high-temperature conditions, Energy Fuel. 31 (2017) 8764–8775, https://doi.org/10.1021/acs.energyfuels.7b00521.

[33] S. Velusamy, S. Sakthivel, J.S. Sangwai, Effect of imidazolium-based ionic liquids on the interfacial tension of the alkane–water system and its influence on the wettability alteration of quartz under saline conditions through contact Angle measurements, Ind. Eng. Chem. Res. 56 (2017) 13521–13534, https://doi.org/10.1021/acs.iecr.7b02528.

[34] Y.F. Hu, T.M. Guo, Effect of the structures of ionic liquids and alkylbenzene-derived amphiphiles on the inhibition of asphaltene precipitation from CO 2-injected reservoir oils, Langmuir 21 (2005) 8168–8174, https://doi.org/10.1021/la050212f.

[35] C. Wang, L. Guo, H. Li, Y. Wang, J. Weng, L. Wu, Preparation of simple ammonium ionic liquids and their application in the cracking of dialkoxypropanes, Green Chem. 8 (2006) 603, https://doi.org/10.1039/b600041j.

[36] S. Aben, C. Holtze, T. Tadros, P. Schurtenberger, Rheological investigations on the creaming of depletion-flocculated emulsions, Langmuir 28 (2012) 7967–7975, https://doi.org/10.1021/la300221m.

[37] M.T. Ghannam, N. Esmail, Yield stress behavior for crude oil–polymer emulsions, J. Petrol. Sci. Eng. 47 (2005) 105–115, https://doi.org/10.1016/J.PETROL.2005.03.001.

[38] N. Aske, A. Harald Kallevik, J. Sjöblom, Determination of saturate, aromatic, resin, and asphaltenic (SARA) components in crude oils by means of infrared and near-infrared spectroscopy. https://doi.org/10.1021/EF010088H, 2001.

[39] N.F. Nejad, E. Shams, M. Adibi, A.A. Miran Beigi, S.K. Torkestani, Desulfurization from model of gasoline by extraction with synthesized [BF 4] – - and [PF 6] – -based ionic liquids, Petrol. Sci. Technol. 30 (2012) 1619–1628, https://doi.org/10.1080/10916466.2010.509071.

[40] S. Banerjee, R. Kumar, A. Mandal, T.K. Naiya, Use of a novel natural surfactant for improving flowability of indian heavy crude oil, Petrol. Sci. Technol. 33 (2015) 819–826, https://doi.org/10.1080/10916466.2015.1014961.

[41] R. Kumar, S. Banerjee, N. Kumar, A. Mandal, T. Kumar Naiya, Comparative studies on synthetic and naturally extracted surfactant for improving rheology of heavy crude oil, Petrol. Sci. Technol. 33 (2015) 1101–1109, https://doi.org/10.1080/10916466.2015.1044612.

[42] X. Huang, M.H. Garcia, A Herschel–Bulkley model for mud flow down a slope, J. Fluid Mech. 374 (1998) 305–333, https://doi.org/10.1017/S0022112098002845.

[43] L.G. Torres, R. Iturbe, M.J. Snowden, B.Z. Chowdhry, S.A. Leharne, Preparation of o/w emulsions stabilized by solid particles and their characterization by oscillatory rheology, Colloids Surfaces A Physicochem. Eng. Asp. 302 (2007) 439–448, https://doi.org/10.1016/J.COLSURFA.2007.03.009.

[44] H.A. Barnes, Applied rheology, Appl. Rheol. 29 (2000) 248–253. https://www.complexfluids.ethz.ch/cgi-bin/AR/ar_contents?DC=1&DOI=10.3933/ApplRheol-10-248&human=yes. (Accessed 9 December 2019). accessed.

[45] C. Jian, T. Tang, S. Bhattacharjee, Probing the effect of side-chain length on the aggregation of a model asphaltene using molecular dynamics simulations, Energy Fuel. 27 (2013) 2057–2067, https://doi.org/10.1021/ef400097h.

[46] R.A. Kumar, N. Papaïconomou, J.M. Lee, J. Salminen, D.S. Clark, J.M. Prausnitz, In vitro cytotoxicities of ionic liquids: effect of cation rings, functional groups, and anions, Environ. Toxicol. 24 (4) (2009) 388–395, https://doi.org/10.1002/tox.20443.

[47] M. Cvjetko Bubalo, K. Radošević, I. Radojčić Redovniković, J. Halambek, V. Gaurina Srček, A brief overview of the potential environmental hazards of ionic liquids, Ecotoxicol. Environ. Saf. 99 (2014) 1–12, https://doi.org/10.1016/j.ecoenv.2013.10.019.

[48] D.O. Hartmann, C.S. Pereira, Toxicity of ionic liquids: past, present, and future, in: Ionic Liquids in Lipid Processing and Analysis, Oppor. Challenges, 2016, pp. 403–421.

[49] S. Stolte, M. Matzke, J. Arning, A. Böschen, W.R. Pitner, U. Welz-Biermann, B. Jastorff, J. Ranke, Effects of different head groups and functionalised side chains on the aquatic toxicity of ionic liquids, Green Chem. (2007), https://doi.org/10.1039/b711119c.